Cancer Research

The PARP Inhibitor AZD2461 Provides Insights into the Role of PARP3 Inhibition for Both Synthetic Lethality and Tolerability with Chemotherapy in Preclinical Models

Lenka Oplustil O'Connor[1], Stuart L. Rulten[2], Aaron N. Cranston[3], Rajesh Odedra[1], Henry Brown[1], Janneke E. Jaspers[4,5], Louise Jones[3], Charlotte Knights[3], Bastiaan Evers[5], Attilla Ting[1], Robert H. Bradbury[1], Marina Pajic[4], Sven Rottenberg[4], Jos Jonkers[5], David Rudge[1], Niall M.B. Martin[3], Keith W. Caldecott[2], Alan Lau[1], and Mark J. O'Connor[1]

Abstract

The PARP inhibitor AZD2461 was developed as a next-generation agent following olaparib, the first PARP inhibitor approved for cancer therapy. In *BRCA1*-deficient mouse models, olaparib resistance predominantly involves overexpression of P-glycoprotein, so AZD2461 was developed as a poor substrate for drug transporters. Here we demonstrate the efficacy of this compound against olaparib-resistant tumors that overexpress P-glycoprotein. In addition, AZD2461 was better tolerated in combination with chemotherapy than olaparib in mice, which suggests that AZD2461 could have significant advantages over olaparib in the clinic. However, this superior toxicity profile did not extend to rats. Investigations of this difference revealed a differential PARP3 inhibitory activity for each compound and a higher level of PARP3 expression in bone marrow cells from mice as compared with rats and humans. Our findings have implications for the use of mouse models to assess bone marrow toxicity for DNA-damaging agents and inhibitors of the DNA damage response. Finally, structural modeling of the PARP3-active site with different PARP inhibitors also highlights the potential to develop compounds with different PARP family member specificity profiles for optimal antitumor activity and tolerability. *Cancer Res; 76(20); 6084–94. ©2016 AACR.*

Introduction

Inhibitors of the DNA damage response (DDR) offer an exciting opportunity to identify targeted cancer therapies (1–3). In addition to enhancing the effectiveness of DNA-damaging chemotherapies and ionizing radiation (IR) treatment, DDR inhibitors have potential for single-agent activity in specific tumor genetic backgrounds based on the principle of synthetic lethality (4). This was first exemplified by inhibitors of the DDR protein PARP in breast cancer associated (*BRCA*)-deficient genetic backgrounds that are associated with a high lifetime risk of breast and ovarian cancer (5, 6).

The mechanism for this single-agent activity has been linked to the role of PARP in the repair of DNA single-strand and double-strand breaks (SSB and DSB; refs. 7–10). After inhibitor treatment, PARP is trapped onto unrepaired SSB, resulting in a protein–DNA adduct (11) that impedes replication fork progression, leading to replication fork collapse and generation of the more genotoxic DSBs. These DSBs would normally be repaired by the homologous recombination repair (HRR) pathway (12), in which *BRCA1* and *BRCA2* genes play pivotal roles (13). However, in tumors with HRR-defective backgrounds (e.g., because of BRCA deficiency), error-prone DNA repair pathways are utilized (9, 10, 14), resulting in accumulation of genomic instability, chromosomal aberrations, and subsequently, cancer cell death.

Olaparib (AZD2281), an oral potent inhibitor of PARP activity (15), is the first PARP inhibitor to gain regulatory approval (16, 17). Olaparib demonstrates low nanomolar activity against PARP1 and PARP2 enzymes and weak enzyme activity against tankyrase-1 (15). Most detectable poly(ADP) ribosylation in mammalian cells is attributed to PARP1 (18), the key PARP protein involved in SSB repair, with PARP2 recognizing gaps and flap structures (19).

Olaparib has demonstrated single-agent antitumor activity in patients with both *BRCA*-mutant ovarian (20) and breast cancer (21), as well as in the broader serous ovarian cancer patient population, where patients without *BRCA* mutations have gained

[1]AstraZeneca, Alderley Park, Macclesfield, United Kingdom. [2]Genome Damage and Stability Centre, University of Sussex, Falmer, Brighton, United Kingdom. [3]KuDOS Pharmaceuticals Ltd, Cambridge, United Kingdom. [4]Division of Molecular Oncology, The Netherlands Cancer Institute, Amsterdam, the Netherlands. [5]Division of Molecular Pathology, The Netherlands Cancer Institute, Amsterdam, the Netherlands.

Note: Supplementary data for this article are available at Cancer Research Online (http://cancerres.aacrjournals.org/).

Current address for L. Oplustil O'Connor and M.J. O'Connor: AstraZeneca, Cambridge, United Kingdom; current address for S. Rottenberg: Institute of Animal Pathology, Vetsuisse Faculty, University of Bern, Bern, Switzerland; and current address for M. Pajic, Personalised Cancer Therapeutics, Garvan Institute of Medical Research, The Kinghorn Cancer Centre, Darlinghurst, New South Wales, Australia.

Corresponding Author: Mark J. O'Connor, Oncology iMED, AstraZeneca, Hodgkin Building (B900), Chesterford Research Park, Little Chesterford, Saffron Walden, CB10 1XL, United Kingdom. Phone: 44-79-1959-6445; Fax: 44-16-2551-5182; E-mail: mark.j.oconnor@astrazeneca.com

doi: 10.1158/0008-5472.CAN-15-3240

clinical benefit (22, 23). In this latter population, olaparib demonstrated a significant increase in progression-free survival (PFS) compared with placebo in patients with high-grade serous ovarian cancer in a maintenance setting. Olaparib was well tolerated as a single agent and cessation of treatment was primarily due to tumor progression, most likely as a consequence of emerging tumor resistance.

Resistance mechanisms associated with olaparib in the clinical setting are poorly understood. Preclinically, reactivation of *BRCA2* gene reading frames by secondary mutations (24) and loss of 53BP1 (25, 26) or REV7 (27) in *BRCA1*;p53-deficient cancer cells have been identified in *BRCA*-deficient tumors. Loss of 53BP1 causing resistance to PARP inhibition has been demonstrated in *BRCA1*-deficient mouse mammary tumors (28) and is suggested to result from 53BP1-deficient KB1PM cells partially restoring HR-mediated DNA repair as evidenced by the presence of DNA damage-induced RAD51 foci (28). Another mechanism of olaparib resistance is overexpression of *Abcb1a* and *Abcb1b* genes encoding the mouse drug efflux transporter P-glycoprotein (P-gp), for which olaparib is a substrate. Overexpression of the *Abcb1a* and *Abcb1b* genes has been described in both *BRCA1*;p53-deficient (29) and *BRCA2*;p53-deficient (30) mouse mammary tumors. While the clinical significance of P-gp–based resistance for olaparib is unclear, it may be of relevance in cancers that are more commonly associated with high P-gp levels, for example, colorectal cancers and acute leukemias.

Here, we characterize a next-generation PARP inhibitor, AZD2461, derived from the same chemical series as olaparib, which retains the same level of anticancer cell potency (*in vitro* and *in vivo*) but is differentiated from olaparib in terms of sensitivity to drug resistance mechanisms and PARP inhibitor profile.

Materials and Methods

Olaparib and AZD2461 PARP inhibitor compounds

The PARP inhibitor olaparib (AZD2281, KU-59436) has been described previously (15). AZD2461 synthesis is described in the international patent WO2009/093032, specifically compound numbers 2b and 47. Formulation of compounds for *in vivo* studies is provided in the Supplementary Material.

Cell line and culture methods

All human cancer cells apart from those stated below were obtained from ATCC (2005–2010). SUM1315MO2 and SUM149PT were purchased from Asterand plc (2005–2010), human cervical cell lines HeLa KB31 and KBA1 cell lines were obtained from DSMZ (2005–2010). All cell lines were authenticated by AstraZeneca using short tandem repeat (STR) profiling. Cell lines were grown in culture media conditions described in the Supplementary Material and maintained as recommended. *BRCA1* mutation status of breast cell lines has been described previously (31).

Alkaline comet assay

The alkaline comet assay was conducted in A549 cells as described in the Supplementary Material. SSBs (tail moments) were analyzed and scored from 100 cells per experiment using Comet Assay IV (Perceptive Instruments; ref. 32). Two-way ANOVA was carried out on the mean values for each time point from replicate experiments.

Immunofluorescence

For γH2AX analysis, a marker of DSB damage, A549 cells were preincubated with DMSO or PARP inhibitors, and then irradiated (2 Gy). Cells were then incubated for specific times to allow repair and immunostained for γH2AX foci, which were counted microscopically. For more details, see the Supplementary Material.

PARP1, PARP2, and tankyrase-isolated enzyme *in vitro* assays

The activity (IC_{50}) of PARP inhibitors was assessed against purified PARP1, PARP2, and tankyrase enzymes *in vitro* as described previously (15).

PARP3 Bio-NAD *in vitro* assay

PARP3 protein was prepared as described previously (33). Ribosylation reaction mix was incubated with Bio-NAD+ (Trevigen) and Sau3A-cut peGFP-C1 plasmid (Clontech). Products were separated by SDS-PAGE, blotted onto nitrocellulose membrane, and signal detected using Streptavidin-HRRP (GE Healthcare). A detailed protocol of the assay is described in the Supplementary Material.

Clonogenic and cell proliferation assays

Cell suspensions were prepared and seeded in recommended dilutions into 6-well plates in triplicate overnight as described in the Supplementary Material. Plates were incubated with olaparib and AZD2461 (0–10 μmol/L) until colonies of >50 formed. Colonies were then visualized by Giemsa staining and scored using Colcount software (Oxford Optronix; see Supplementary Material). Cellular IC_{50} values were determined for each cell line using Microsoft Excel and ID-BS XLfit (v4.2.2) charting application.

For sulphorhodamine B (SRB) assay, cells were seeded into 96-well plates (6,000 cells/well) in triplicate and preincubated with AZD2461 or olaparib (0–200 nmol/L) for 1 hour prior to addition of methyl methanesulfonate (MMS; 0–15 μg/mL). Cells were incubated, fixed, and stained as described in the Supplementary Material. Absorbance was determined at 564 nmol/L. Data are presented as percentage cell growth relative to untreated control. Cellular PF_{50} (potentiation factor at 50% cell survival) was calculated as the ratio of the IC_{50} for MMS alone versus MMS in combination with single concentrations of PARP inhibitors.

Rodent experiments

Brca1$^{\Delta 5\text{-}13/\Delta 5\text{-}13}$;*p53*$^{\Delta 2\text{-}10/\Delta 2\text{-}10}$ mammary tumors were generated in *K14cre*;*Brca1*$^{F5\text{-}13/F5\text{-}13}$;*p53*$^{F2\text{-}10/F2\text{-}10}$ mice and genotyped as described previously (34). Orthotopic transplantations of tumor fragments into syngeneic animals and caliper measurements of mammary tumors have been previously reported, along with generation of the olaparib-resistant tumor T6-28 (29). Treatments were started when tumor volume reached about 200 mm^3 ($V = \text{length} \times \text{width}^2/2$). Olaparib [50 mg/kg intraperitoneally (i.p.)], tariquidar (2 mg/kg i.p.), or AZD2461 (100 mg/kg orally) were given daily. Tariquidar was administered 30 minutes before olaparib.

Mice (CD-1 Nude *Foxn1*^{nu}, Charles River Laboratories) were orally dosed once daily for 5 days with the combination therapies temozolomide (50 mg/kg) plus either olaparib (10 mg/kg) or AZD2461 (10 mg/kg) followed by once-daily dosing of olaparib or AZD2461 for an additional 2 days. Rats (HsdHan:RNU-*Foxn1*^{rnu}) were dosed orally once daily for 5 days with single

agents or combination therapies (temozolomide 50 mg/kg, olaparib 10 and 20 mg/kg, or AZD2461 10 and 20 mg/kg). During the dosing phase, animals were weighed daily. Mice were culled for bone marrow analysis as described in the Supplementary Material. All experimental procedures were carried out according to current UK Home Office regulations.

Flow cytometry analysis of bone marrow cells

Bone marrow cells were prepared from rodent femurs as described in the Supplementary Material and samples analyzed on a flow cytometer (FACSCanto, BD Biosciences) using forward (FSC-H) and side scatter (SSC-H) on linear scales.

RNA isolation and RT-PCR

Total RNA was extracted from fresh bone marrow of 6 individual mice (CD-1 Nude *Foxn1*^{nu}), 6 rats (HsdHan:RNU-*Foxn1*^{rnu}), and human bone marrow mononuclear cells from six different individuals (Lonza 2M-125C) using RNeasy Mini kit (Qiagen) according to the manufacturers' instructions (see Supplementary Material including assessment of RNA purity and concentration). Human, rat, and mouse PARP1, 2, and 3 sequences were aligned using the Megalign module in DNAstar to facilitate the design of primers and probes for TaqMan and SYBR Green qRT-PCR assays in areas of sequence identity. Primers and probes were custom or catalog ordered from Life Technologies (Invitrogen; see Supplementary Material for sequences and qRT-PCR assay analysis).

Results and Discussion

Development of the next-generation PARP inhibitor, AZD2461

We set about identifying a compound with similar efficacy to olaparib but without the potential liability associated with being a substrate for the P-gp (MDR1) transporter. Triaging of compounds following medicinal chemistry (see Supplementary Material) identified two series of compounds around the phthalazinone core of olaparib. AZD2461 (Fig. 1A) was identified as the optimal compound from the Piperidine Ether series (see international patent WO2009/093032, specifically compound number 2b and 47) and is a potent inhibitor of both PARP1 and PARP2 with IC_{50} values of 5 nmol/L and 2 nmol/L, respectively, comparable with olaparib (5 nmol/L and 1 nmol/L, respectively). The lack of selectivity between PARP1 and PARP2 may be a positive feature when attempting to inhibit SSB repair, as PARP2 also plays an important role in this pathway (35). Both AZD2461 and olaparib were effective at inhibiting formation of cellular poly (ADP-ribose) (PAR) polymers following treatment with 10 mmol/L hydrogen peroxide (Supplementary Fig. S1). The alkaline COMET assay, where the length of the comet tail moment represents the degree of unrepaired SSBs following induction of DNA damage by IR, was used to confirm that observed PAR inhibition translated into inhibition of SSB repair (Fig. 1B). In addition, AZD2461 potentiated the antiproliferation effect of the DNA-damaging alkylating agent MMS, which induces SSBs (Fig. 1C; Supplementary Table S1). Collectively, these data confirm that AZD2461 is as effective at inhibiting SSB repair as olaparib.

Activity against *BRCA*-deficient tumors through synthetic lethality is a key component of olaparib's developmental program. Thus, we sought to determine the potency of single-agent AZD2461 in *BRCA*-deficient cancer cells. *In vitro* clonogenic assays were performed with AZD2461 and olaparib against a panel of breast cancer tumor cells with either mutant (MDA-MB-436, SUM1315MO2, and SUM149PT) or wild-type (WT; T47D, BT549, and MDA-MB-231) *BRCA1* gene status. Both olaparib and AZD2461 exhibited similar pharmacokinetic and pharmacodynamic profiles (see Supplementary Material and Supplementary Fig. S2) and significant potency as single agents in the *BRCA1*-mutant breast cancer cell lines but not in the *BRCA1* WT cell lines (Fig. 1D).

Assessment of the *in vitro* permeability and efflux of AZD2461 was undertaken in the human intestinal-derived cell line CaCo-2 (see Supplementary Material and Supplementary Table S2) and in the matched cell lines KBA1, a genetically modified version of HeLa that overexpresses high levels of P-gp (36), and KB31, which does not overexpress P-gp (Fig. 2A). While this functional assay does not distinguish between saturation of the P-gp pumps versus low binding, it does discriminate between compounds that are highly effluxed and those that are not. Using these assays, we were able to distinguish low versus highly effluxed compounds, while addition of the P-gp inhibitor verapamil provided further evidence that efflux was occurring through a P-gp mechanism. The data in Fig. 2A show that, in contrast to olaparib, AZD2461 has similar activity between KBA1 cells and matched WT KB31 cells and addition of verapamil to KBA1 cells showed little effect on the cellular activity of AZD2461, indicating that AZD2461 is significantly less prone to P-gp–mediated efflux mechanisms than olaparib. Similar data supporting a lack of P-gp liability in AZD2461 were obtained in the colorectal cancer cell line HCT-15, which expresses high levels of endogenous P-gp (Supplementary Fig. S3 and Supplementary Table S3).

To assess AZD2461 activity in a more clinically relevant *BRCA*-mutant background and acquired resistant setting, we used *in vitro* and *in vivo* models where prolonged olaparib treatment had led to resistance and high P-gp expression levels. The *BRCA2*-deficient mouse breast cancer line KB2P3.4 was generated from a *BRCA2*-deficient mouse mammary tumor that demonstrated sensitivity to olaparib treatment (37). This cell line was treated in culture with olaparib for 2 months to induce the olaparib-resistant line KB2P3.4R, and overexpression of P-gp was confirmed using immunofluorescence with a P-gp antibody (Fig. 2B). Treatment of the parental KB2P3.4 with AZD2461 resulted in a similar response to olaparib (Fig. 2B). However, unlike olaparib, AZD2461 was also effective in the KB2P3.4R cell line. Consistent with this difference being based on P-gp, olaparib sensitivity in KB2P3.4R cells was restored on cotreatment with tariquidar, a new generation P-gp inhibitor.

Increased expression of *Abcb1a* and *Abcb1b* encoding the mouse drug efflux transporter P-gp contributes to olaparib resistance in *BRCA1*;p53-deficient mouse mammary tumors (29). To determine whether AZD2461 could overcome olaparib resistance *in vivo*, small tumor fragments of an olaparib-resistant tumor (T6-28) exhibiting an 80-fold increased expression of *Abcb1b* were transplanted into syngeneic WT female mice and treated with olaparib, combination olaparib and tariquidar, or AZD2461. As expected, olaparib resistance was successfully overcome by tariquidar pretreatment (Fig. 2C). Tumors were sensitive to AZD2461 in the absence of tariquidar, consistent with the idea that spontaneous *BRCA1*;p53-defective mammary tumors, in which resistance is caused by increased P-gp-mediated drug efflux, remain sensitive to AZD2461. Moreover, in a separate study, long-term AZD2461 treatment in the *BRCA1*;p53-defective mouse tumor model suppressed development of drug resistance (28).

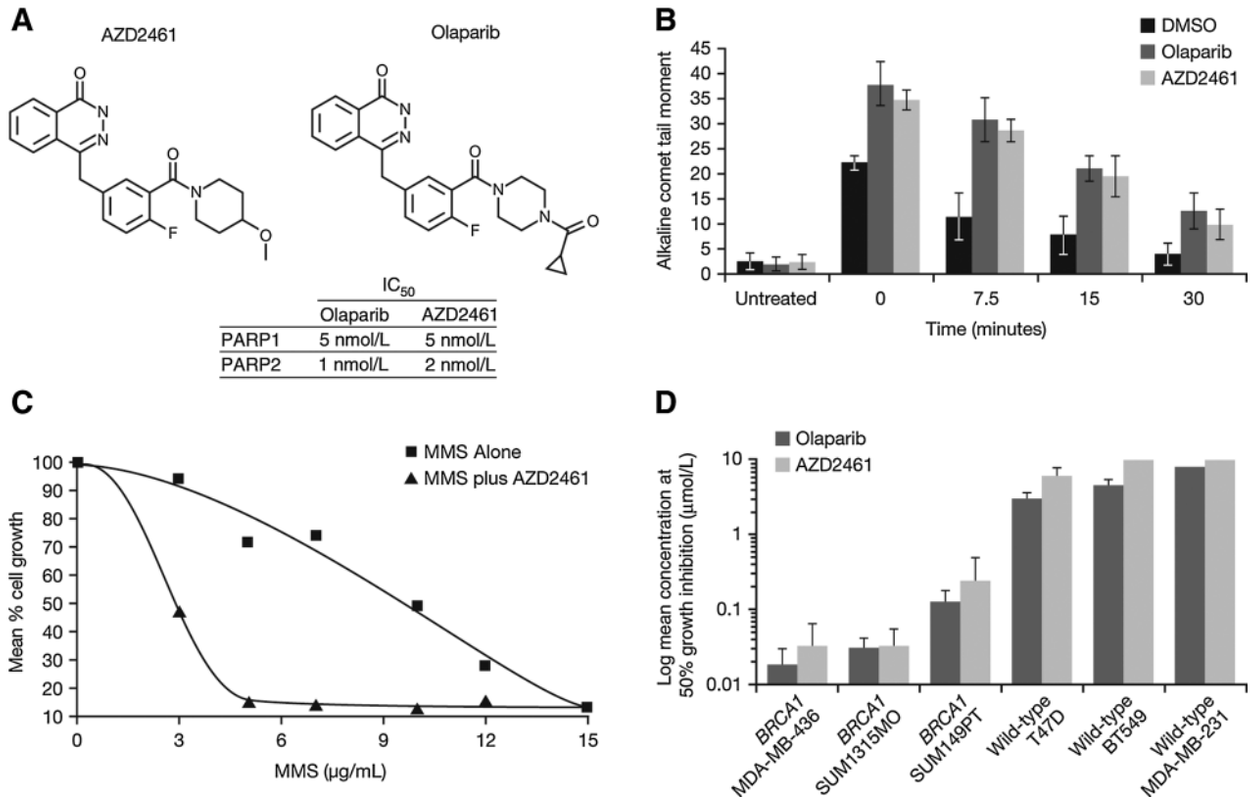

Figure 1.

AZD2461 has comparable effects on DNA single-strand break repair and efficacy as olaparib *in vitro*. **A,** chemical structure of AZD2461 and olaparib and respective enzymatic IC_{50} against PARP1 and PARP2. **B,** alkaline comet assay to assess SSB repair in human A459 cells following preexposure to olaparib or AZD2461 (500 nmol/L for both), followed by IR treatment (data from three independent results). **C,** SRB assay to assess potentiality effects of AZD2461 on MMS in HeLa cells. **D,** clonogenic survival assay to assess single-agent activity of AZD2461 and olaparib and corresponding IC_{50} values in *BRCA1*-deficient breast cancer cell lines (MDA-MB-436, SUM1315MO2, and SUM149PT), and wild-type *BRCA1* breast cancer lines (T47D, BT549, and MDA-MB-231). IC_{50} values >10 μmol/L are shown as = 10 μmol/L (data from three independent experiments).

Together, these data demonstrate that AZD2461 is a potent inhibitor of PARP1 and PARP2 that can provide effective inhibition of SSB repair and has significant single-agent activity in *BRCA*-deficient cancer cells, comparable with olaparib. Moreover, we have shown that AZD2461 is a poor substrate for P-gp and has activity in olaparib-resistant cancer cells that overexpress P-gp *in vitro* and is capable of antitumor activity *in vivo* in olaparib-resistant tumors where resistance is based on overexpression of P-gp. Accordingly, the goal to develop a follow-on compound to olaparib, that has comparable activity but without P-gp liability, has been successful. AZD2461, therefore, represents an excellent preclinical tool to study PARP inhibitor resistance and may help identify additional mechanisms of PARP inhibitor resistance.

AZD2461 is as efficacious as, and better tolerated than, olaparib in combination with temozolomide in a mouse xenograft model

In addition to the utility of PARP inhibitors as single agents, there is a strong rationale for combination with DNA-damaging chemotherapies, such as temozolomide or camptothecins that induce SSBs (38, 39). As a single agent, synthetic lethality of olaparib relies on endogenously generated SSBs and the inability of *BRCA* mutation or other HRR deficiency to repair the ensuing DSBs, ultimately resulting in cancer cell death. In combination with DNA-damaging chemotherapies, the number of SSBs generated by the chemotherapy agent is much larger than those that occur endogenously (40). If repair is prevented (e.g., by PARP inhibitor treatment), cell death can be induced even when the HRR pathway is functional, purely because the tolerated DNA damage threshold is exceeded. This has two important implications: first, combination of a PARP inhibitor and SSB-inducing agent can result in killing HRR-proficient as well as HRR-deficient cancer cells; second, potential for damage in normal tissue compartments is increased, as evidenced in the increased hematologic toxicities observed when PARP inhibitors and alkylating agents are combined (41).

To assess AZD2461 in combination with temozolomide *in vivo*, we used a mouse colorectal xenograft (SW620) model to compare antitumor activity of 50 mg/kg temozolomide given once daily for 5 days either alone or in combination with AZD2461 or olaparib (both at 10 mg/kg for 7 days). This dose and schedule of olaparib had previously demonstrated potentiation of temozolomide antitumor activity (Supplementary Fig. S4). The data presented in Fig. 3A show that temozolomide alone demonstrated antitumor activity and this improved when combined with a PARP

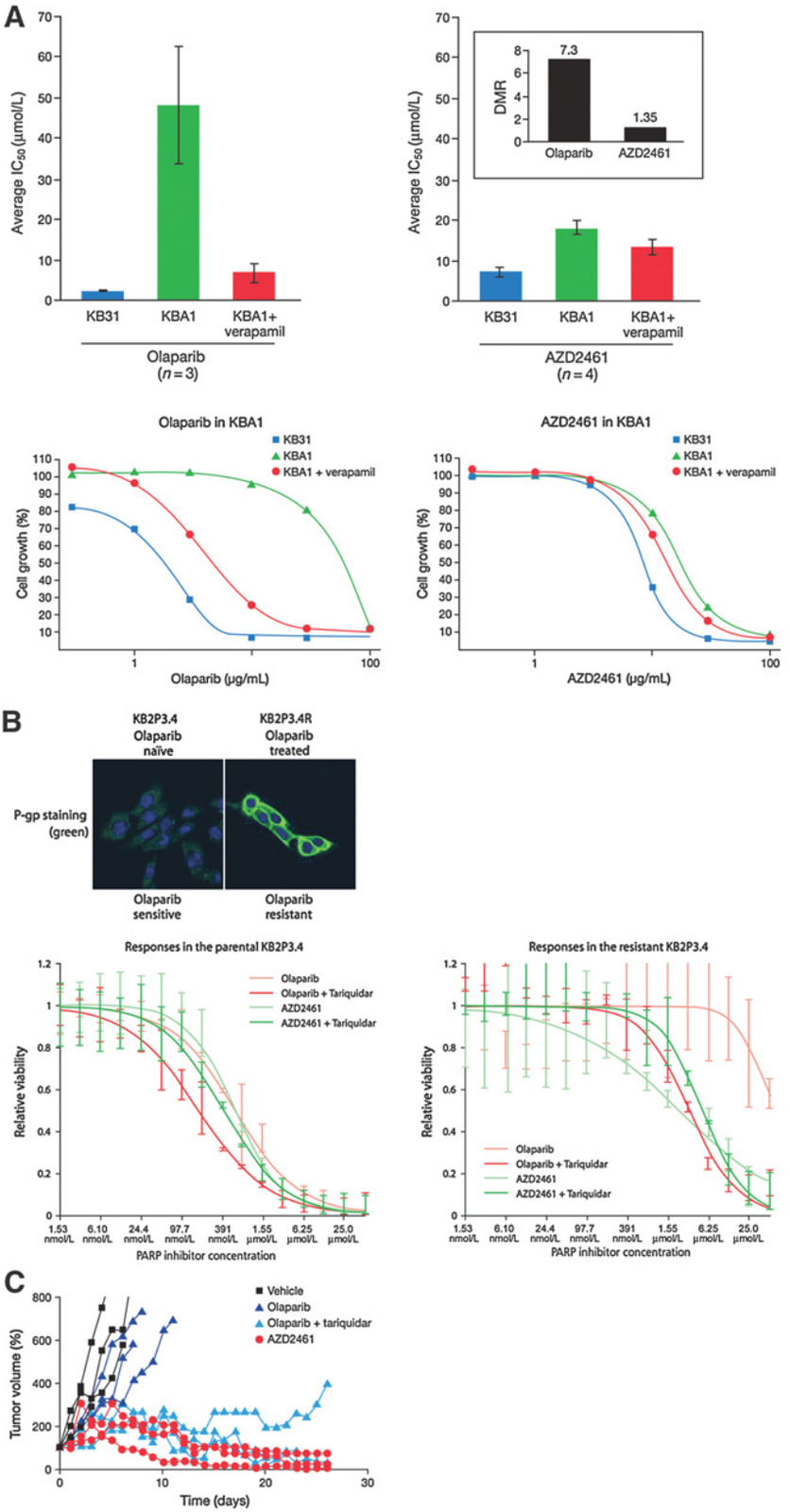

Figure 2.

AZD2461 overcomes P-gp–associated resistance to olaparib. **A,** activity of AZD2461 and olaparib in matched cell lines, KBA1 cells (a genetically modified version of HeLa that overexpresses high levels of P-gp) and KB31 cells. **B,** immunofluorescence staining for P-gp and relative growth inhibition following treatment with olaparib or AZD2461 with and without tariquidar in the parental KB2P3.4 BRCA2$^{-/-}$ mouse cell line and an acquired olaparib-resistant clone KB2P3.4R. **C,** response of the olaparib-resistant *Brca1*$^{\Delta 5\text{-}13/\Delta 5\text{-}13}$;*p53*$^{\Delta 2\text{-}10/\Delta 2\text{-}10}$ tumor T6-28 to AZD2461. Animals carrying transplanted tumors were treated daily with 0.5% HPMC (vehicle) 10 mL/kg orally, AZD2461 100 mg/kg orally, and olaparib 50 mg/kg i.p. with and without tariquidar 2 mg/kg i.p. (tumor volume day 0, 100%).

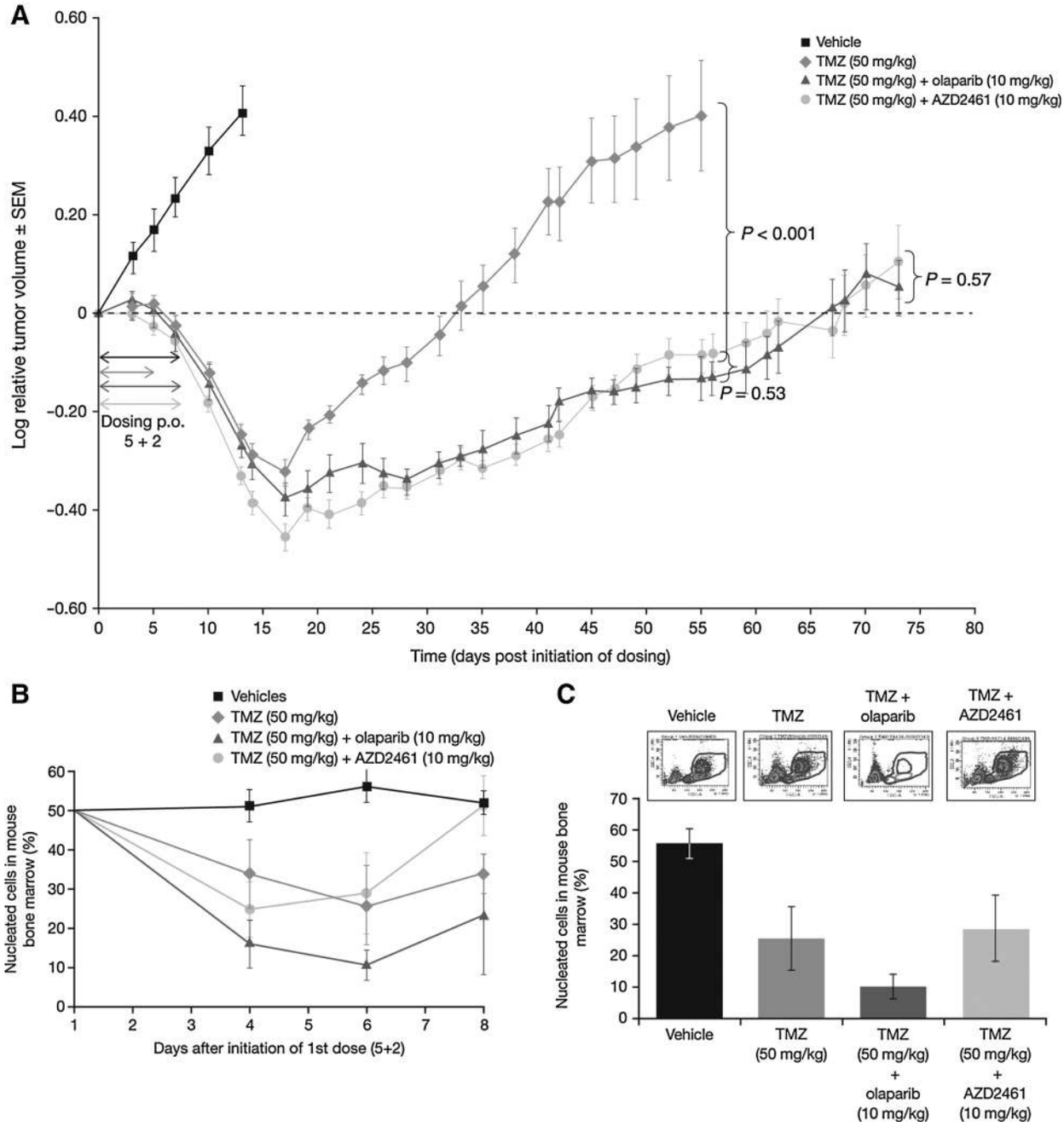

Figure 3.

AZD2461 is as effective as olaparib in potentiating the antitumor efficacy of temozolomide and shows lower impact on mouse bone marrow cells. **A,** antitumor activity of AZD2461 or olaparib (7 days each) in combination with temozolomide (5 days) in an SW620 tumor xenograft model. Tumor volumes were plotted relative to the first day of dosing. Comparisons were made to the single-agent temozolomide (one-sided) and between the combination AZD2461 and olaparib groups (two-sided) employing Student *t* test comparisons with pooled inter-animal variability. **B,** kinetics of nucleated cells in mouse bone marrow following treatment with AZD2461 and olaparib in combination with temozolomide. Samples were analyzed 24 hours after the third, fifth, and seventh dose. **C,** mouse bone marrow analysis showing the effects of temozolomide with and without olaparib or AZD2461 on the total population of nucleated cells. p.o., orally

inhibitor. This difference was statistically significant ($P < 0.001$) at day 55 (when the temozolomide group was culled); the effect between the combination groups (i.e., temozolomide plus olaparib or AZD2461) was not statistically significant either at day 55 ($P = 0.53$) or when the study was stopped at day 73 ($P = 0.57$). Both combination treatments conferred considerable delay in tumor regrowth compared with temozolomide alone.

We examined body weight loss as a gross indicator of tolerability and myelosuppression as a more clinically relevant indicator of combinatorial toxicity. Body weights of mice decreased relative to their weight at the start of the experiment but recovered quickly after the dosing was finished; weight loss was greater in the two combination groups versus the temozolomide alone group (Supplementary Fig. S5).

To assess the impact of the combinations on bone marrow populations, we examined cohorts of mice given the same dose regimens as used in the combination efficacy study. Mice were culled at time points across the dosing phase to create a time course in which the impact of treatments on bone marrow cells could be assessed (Fig. 3B and C). Flow cytometry identified three distinct white blood cell populations (lymphocytes, monocytes, and neutrophils). Temozolomide alone led to a reduction in the total number of white blood cells in bone marrow with the nadir after the last dose and a failure to return to starting levels at day 8. Temozolomide in combination with olaparib led to a significantly greater impact on bone marrow (a nadir at day 6 and a worse state of recovery at day 8).

An unexpected finding, however, was that combination AZD2461 and temozolomide did not result in the same severity of bone marrow effects as the olaparib combination. The nadir was not statistically different from temozolomide alone and there was a good recovery by day 8. Although lower doses of olaparib could result in less bone marrow toxicity, these are also likely to be less efficacious, as demonstrated by Supplementary Fig. S4, which shows that doses $\leq$3 mg/kg of olaparib in combination with temozolomide (50 mg/kg) do not confer a statistically significant benefit over temozolomide alone (MTD 68 mg/kg).

Collectively, these data suggest that AZD2461 might have two potential advantages over olaparib. First, while having a similar level of antitumor activity, AZD2461 did not have the same level of P-gp liability as olaparib; second, AZD2461 appeared better tolerated in combination with a DNA-damaging chemotherapy. The basis for this latter observation, though, cannot be attributed to PARP1/PARP2 inhibition, as both treatments are similar in this respect, suggesting an as yet unidentified mechanism.

AZD2461 and olaparib have differential activity against PARP3

One possible explanation for the hematologic toxicity differences observed between olaparib and AZD2461 could be differential PARP3 activity. PARP3 plays an important role in nonhomologous end joining (NHEJ), where it is stimulated by DSBs *in vitro* and functions in the same pathway as the PAR-binding

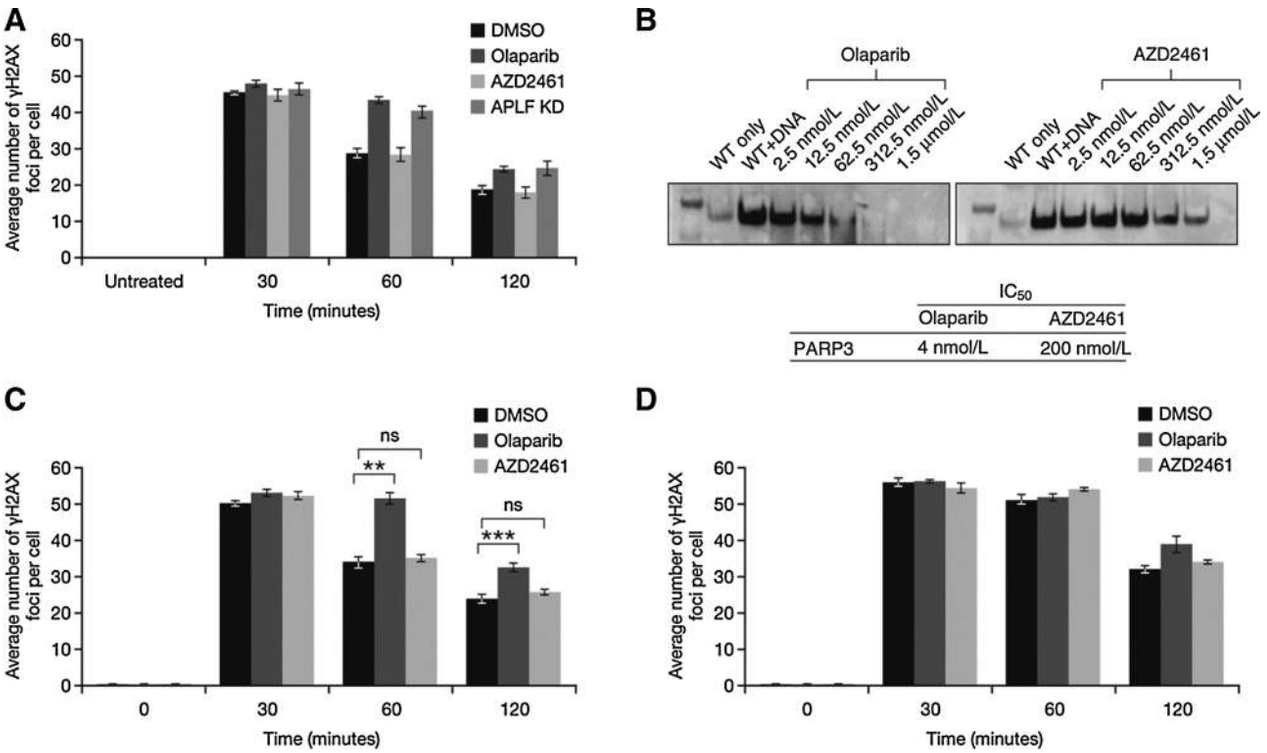

Figure 4.

AZD2461 inhibits PARP3 to a lesser extent than olaparib, resulting in a lack of inhibition of nonhomologous end-joining repair in cancer cells. **A,** repair of DSBs, as assessed by γH2AX immunofluorescence, in human A549 cells. Cells were preincubated with 500 nmol/L AZD2461 or olaparib before IR and allowed to repair for the times indicated. A stable APLF knockdown cell line was used as a control for cells lacking PARP3/APLF-dependent NHEJ (APLF KD; mean ± SEM from four independent experiments). **B,** PARP3 enzyme inhibition assay with olaparib and AZD2461 (2.5 nmol/L–1.5 μmol/L assays used 200 nmol/L PARP3 in the presence of 25 μmol/L Biotin-NAD and 200 ng Sau3AI-cut plasmid. **C** and **D,** repair of DSBs, as assessed by γH2AX immunofluorescence, in primary $PARP3^{+/+}$ (**C**) or $PARP3^{-/-}$ (**D**) mouse embryonic fibroblasts. Cells were pretreated with 500 nmol/L olaparib or AZD2461 before IR and allowed to repair for the indicated times (mean ± SE from four independent experiments). **, $P < 0.01$; ***, $P < 0.0001$ by paired *t* test. ns, nonsignificant.

protein APLF to accelerate chromosomal DSB repair (33). Following IR treatment, γH2AX can be used as a marker of DSB damage (42, 43). The repair of DSBs and the decline in γH2AX over time following IR was abrogated by either the loss of PARP3, APLF, or treatment with the PARP inhibitor KU-58948, which is related chemically to olaparib (33).

The link between PARP3, NHEJ, and mouse bone marrow was highlighted in studies of murine hematopoietic stem and multipotent progenitor cells (HSPC), which were shown to be more resistant to IR-induced damage than more differentiated progenitor cells (44). This difference was based on both an increased resistance to apoptosis and the ability to repair DNA by NHEJ. The NHEJ pathway is a lower fidelity alternative to HRR DSB repair, and mice bone marrow stem cells appear to utilize NHEJ while human HSPCs undergo apoptosis in response to DNA damage (45). It has been suggested that these differences may reflect the different challenges faced by mammals with diverse life spans and ages of reproductive maturity (46).

To investigate whether differential PARP3 activity could provide the basis for the differential hematologic toxicity observed with olaparib and AZD2461 in mice, we looked at the effect of these inhibitors on γH2AX following IR treatment (Fig. 4A). Unlike olaparib, which results in persistence of γH2AX following IR to the same degree as APLF knockdown, AZD2461 had no effect on γH2AX dynamics. To confirm whether this observation was due to PARP3 inhibition, we carried out PARP3 enzyme inhibition assays where PARP3 auto-ADP-ribosylation activity was assessed following the addition of increasing doses (2.5 nmol/L–1.5 μmol/L) of olaparib or AZD2461. Fig. 4B shows that AZD2461 did not inhibit PARP3 to the same extent as olaparib. There was a 50-fold difference in PARP3 inhibitory activity, with the IC_{50} value for PARP3 being 4 nmol/L for olaparib and 200 nmol/L for AZD2461 (Fig. 4B). The data in Fig. 4A, C, and D are consistent with (although not proof of) this difference at the enzyme level being translated into a failure to inhibit NHEJ DSB repair, based on γH2AX kinetics.

Increased bone marrow tolerability of AZD2461 in combination with temozolomide is mouse specific and is not seen in rat models

The finding that AZD2461 does not inhibit PARP3, coupled with previous studies that suggest mouse bone marrow HSPCs preferentially use NHEJ when dealing with DNA damage, suggests our observation of better tolerability of chemotherapy combination could be specific to mice and not translate into humans. Prior to initiating clinical trials to assess combination tolerability, we repeated the experiment in Fig. 3 in an athymic rat model. First, we assessed PARP3 levels (and compared with PARP1 and PARP2 levels) in HSPCs from mice, rats, and humans (Fig. 5 and Supplementary Figs. S6 and S7). PARP3 levels were about 3.7 times higher in mice than in rats (Fig. 5A), consistent with use of NHEJ as a primary repair mechanism. Because of a lack of the same sequence identity, it was not possible to directly compare levels of PARP3 expression across mice, rats, and human bone marrow cells using the TaqMan probe-based assay. However, using SYBR Green dye detection RT-PCR, we designed specific primers for human and rat PARP3 and demonstrated that the relative level of PARP3 expression is similar between rat and human bone marrow cells (Fig. 5B).

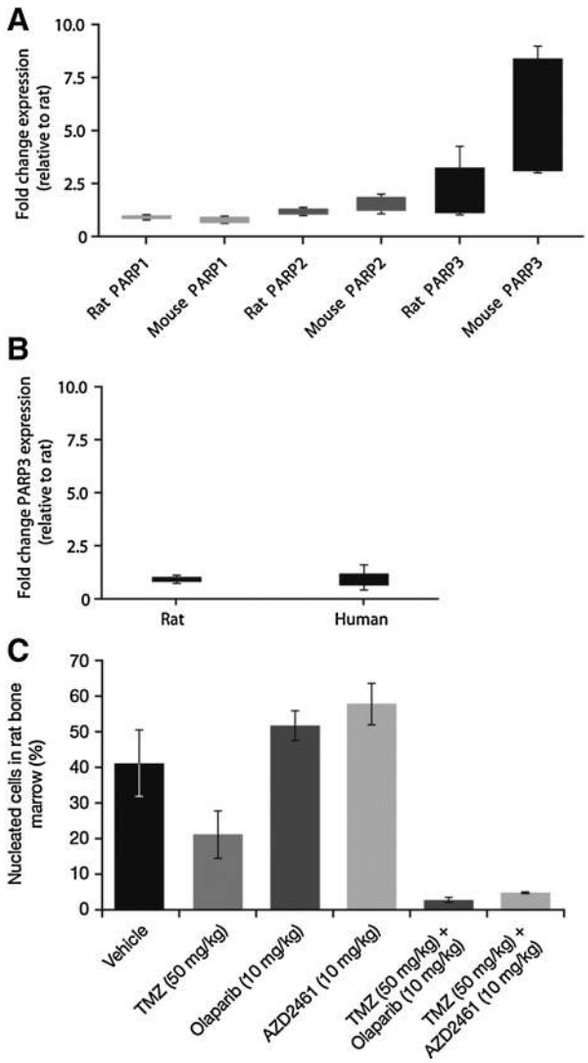

Figure 5.
PARP3 levels are significantly higher in mouse but not rat or human bone marrow cells and, consistent with this, is a lack of differential bone marrow toxicity between AZD2461 and olaparib in rats. **A,** PARP1, PARP2, and PARP3 gene expression in mouse and rat bone marrow cells using customized TaqMan assays (means difference for rat versus mouse, PARP1 = 0.1517, $P = 0.0632$; PARP2 = −0.3883, $P = 0.0318$; PARP3 = −3.717, $P = 0.0169$; $n = 6$ biological samples). **B,** PARP3 gene expression in rat and human bone marrow cells measured using SYBR Green RT-PCR assay (rat versus human PARP3 means difference = −0.01548, $P = 0.9232$; $n = 6$ biological samples). Box-and-whiskers graphs show mean from three experimental repeats. **C,** female athymic rat bone marrow analysis (day 5 of treatment) using flow cytometry analysis as in Fig. 3C. Graph shows mean ± SD of total nucleated cell population (% of parent) in individual treatment groups ($n = 3$).

To increase confidence around the finding of better hematologic tolerability, we repeated the temozolomide combination study in Fig. 3C in an athymic rat model (Fig. 5C). Contrary to the results in mice, AZD2461 was no better tolerated than olaparib in terms of bone marrow toxicity (Fig. 5C) or total body weight loss in rats (Supplementary Fig. S8).

Similar data were obtained in male athymic rats (data not shown). This difference could not be explained by pharmacokinetic differences as these are comparable in mice and rats [10 mg/kg in both cases giving an area under the curve (AUC_t) of 1–2 μmol × h/L].

We have provided an explanation for the better tolerability of AZD2461 compared with olaparib observed in mice by providing data showing the differential PARP3 activity and the different impact of the two compounds on NHEJ DSB repair. To date, technical challenges around the isolation and analysis of rat HSPCs have prevented us from directly demonstrating that rats are different from mice in utilizing NHEJ. Therefore, our explanation for the better tolerability of AZD2461 compared with olaparib in mice being attributable to NHEJ DSB repair mechanisms is based on indirect evidence and we cannot rule out alternative reasons for combination toxicity differences observed between the two rodent species. However, the clinical experience of combining PARP inhibitors with temozolomide (41) does argue that rat and not mouse is the better predictive model.

Structural analysis of the PARP3-active site

Previous studies have made the observation that PARP3 differs from PARP1 and PARP2 in the D-loop structure within the catalytic domain (47). A sequence alignment of this region (Fig. 6 and Supplementary Material) shows that PARP3 contains a shorter loop within this region versus PARP1 and PARP2. A graphical model of the PARP3 crystal structure bound to the PARP inhibitor, KU58948, is shown in Fig. 6, see also (47), with the variant region highlighted. PARP3 may be more restrictive for binding by PARP inhibitors with charged or extended groups beyond the carbonyl linker region of these molecules, whereas the PARP1 and PARP2 structures have a more extended D-loop and may be more permissive for inhibitor binding. Fig. 6 also shows a comparison of the chemical structures of KU58948, olaparib and AZD2461, with variable groups beyond the linker region

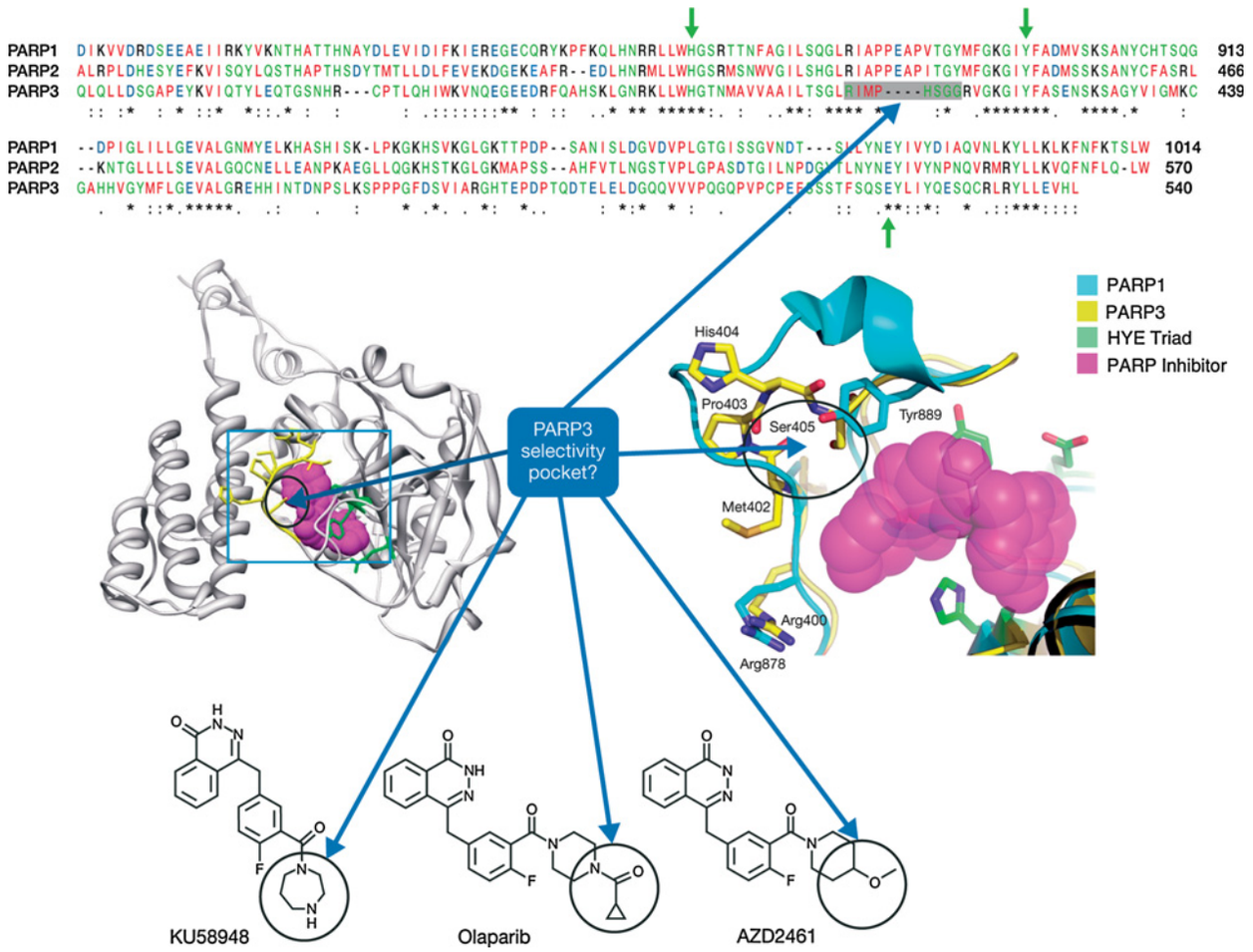

Figure 6.

Comparison between the catalytic domains of PARP1 and PARP3. Sequence alignment of a portion of the catalytic domains of PARPs 1–3. Residues forming the "HYE triad" within the catalytic core (green arrows) and a PARP3-specific deletion (gray box) are shown. The model shows the PARP3 crystal structure bound by the PARP inhibitor KU58948 (magenta) with the putative PARP3 selectivity pocket shown in yellow and "HYE triad" residues in green. Right, a closer image of the PARP inhibitor pocket with the PARP3 variant region in yellow and the corresponding PARP1 structure aligned in cyan. Also shown are the chemical structures of the PARP inhibitors KU58948, olaparib, and AZD2461; variable side chains thought to contribute to PARP3 selectivity are highlighted.

highlighted. This illustrates that derivatives of olaparib could be generated for selectivity for or against PARP3 by targeting the variable region in the PARP3 D-loop structure.

The demonstration of differential PARP3 activity of AZD2461 compared with olaparib has two important ramifications. First, we are just beginning to understand the biological roles of the different PARP family members and their interplay. For example, this study demonstrates that AZD2461 could represent a useful tool to distinguish cellular functions of PARPs 1–3 in DNA repair. Specifically, previous *in vitro* studies have shown that PARP3 preparations can activate PARP1, and it has been suggested that PARP3 plays a role in regulating the DNA damage response through PARP1 activation (48). However, our study shows that in cells treated with AZD2461, PARP3 is likely active in the NHEJ pathway, even in the absence of detectable PARP1 activity, suggesting PARP1 and PARP3 may play independent roles in chromosomal DNA repair. Second, the structural similarity between olaparib and AZD2461 that results in this observed differential activity against PARP3 has allowed a rationalization of the mechanistic basis of this difference in specificity via modeling of the PARP inhibitors in the PARP3-active site.

Increased understanding of inhibitor–PARP family member interactions, as demonstrated by an independent study (49), will also facilitate our understanding of the PARP family biology. Together, advances in both the ability to generate inhibitors with a particular PARP specificity profile, as has been suggested recently (50), along with an understanding of the biological roles of the different PARP family members, should provide the opportunity to generate inhibitors with an optimal PARP inhibitory profile to maximize antitumor activity and therapeutic index.

Disclosure of Potential Conflicts of Interest

No potential conflicts of interest were disclosed.

Authors' Contributions

Conception and design: L. Oplustil O'Connor, S.L. Rulten, A. Ting, S. Rottenberg, D. Rudge, N.M.B. Martin, K.W. Caldecott, A. Lau, M.J. O'Connor

Development of methodology: A.N. Cranston, H. Brown, S. Rottenberg, J. Jonkers, M.J. O'Connor

Acquisition of data (provided animals, acquired and managed patients, provided facilities, etc.): L. Oplustil O'Connor, S.L. Rulten, A.N. Cranston, R. Odedra, J.E. Jaspers, L. Jones, C. Knights, B. Evers, M. Pajic, S. Rottenberg, J. Jonkers

Analysis and interpretation of data (e.g., statistical analysis, biostatistics, computational analysis): L. Oplustil O'Connor, S.L. Rulten, A.N. Cranston, R. Odedra, H. Brown, B. Evers, A. Ting, R.H. Bradbury, M. Pajic, S. Rottenberg, J. Jonkers, N.M.B. Martin, A. Lau, M.J. O'Connor

Writing, review, and/or revision of the manuscript: L. Oplustil O'Connor, A.N. Cranston, R. Odedra, C. Knights, A. Ting, R.H. Bradbury, S. Rottenberg, J. Jonkers, K.W. Caldecott, A. Lau, M.J. O'Connor

Administrative, technical, or material support (i.e., reporting or organizing data, constructing databases): M.J. O'Connor

Study supervision: S.L. Rulten, A. Lau, M.J. O'Connor

Other (his laboratory conducted some of the PARP3 experiments): K.W. Caldecott

Acknowledgments

Tariquidar was a kind gift of Dr. Susan Bates from the NIH. The authors would like to thank Stephen Moore, James Harrison, Gabrielle Grundy, Antony Oliver, Cydney Morgan and Eva Schut for their technical support. Editorial support was provided by Kerry Acheson, PhD, of iMed Comms, Macclesfield, UK, and Martin Goulding, PhD, of Mudskipper Business Ltd., funded by AstraZeneca.

Grant Support

This work was supported by grants from the European Community's Seventh Framework Programme (FP7/2007-2013) under grant agreement no. HEALTH-F2010-259893 (L. Oplustil O'Connor and M.J. O'Connor); the Netherlands Organization for Scientific Research (NWO-Toptalent021.002.104 to J.E. Jaspers; NWO-VIDI-91711302 to S. Rottenberg) and the Dutch Cancer Society (NKI 2007-3772 and NKI 2011-5220 to J. Jonkers and S. Rottenberg), and the CR-UK project grant, C6563/A1307 (S.L. Rulten and K.W. Caldecott). The work was also supported by AstraZeneca.

The costs of publication of this article were defrayed in part by the payment of page charges. This article must therefore be hereby marked *advertisement* in accordance with 18 U.S.C. Section 1734 solely to indicate this fact.

Received December 17, 2015; revised July 20, 2016; accepted July 26, 2016; published OnlineFirst August 22, 2016.

References

1. Curtin NJ. DNA repair dysregulation from cancer driver to therapeutic target. Nat Rev Cancer 2012;12:801–17.
2. Lord CJ, Ashworth A. The DNA damage response and cancer therapy. Nature 2012;481:287–94.
3. O'Connor MJ, Martin NM, Smith GC. Targeted cancer therapies based on the inhibition of DNA strand break repair. Oncogene 2007;26:7816–24.
4. Kaelin WG Jr. The concept of synthetic lethality in the context of anticancer therapy. Nat Rev Cancer 2005;5:689–98.
5. Bryant HE, Schultz N, Thomas HD, Parker KM, Flower D, Lopez E, et al. Specific killing of BRCA2-deficient tumours with inhibitors of poly(ADP-ribose) polymerase. Nature 2005;434:913–7.
6. Farmer H, McCabe N, Lord CJ, Tutt AN, Johnson DA, Richardson TB, et al. Targeting the DNA repair defect in BRCA mutant cells as a therapeutic strategy. Nature 2005;434:917–21.
7. D'Amours D, Desnoyers S, D'Silva I, Poirier GG. Poly(ADP-ribosyl)-ation reactions in the regulation of nuclear functions. Biochem J 1999; 342:249–68.
8. Lindahl T, Satoh MS, Poirier GG, Klungland A. Post-translational modification of poly(ADP-ribose) polymerase induced by DNA strand breaks. Trends Biochem Sci 1995;20:405–11.
9. Ceccaldi R, Liu JC, Amunugama R, Hajdu I, Primack B, Petalcorin MI, et al. Homologous-recombination-deficient tumours are dependent on Poltheta-mediated repair. Nature 2015;518:258–62.
10. Mateos-Gomez PA, Gong F, Nair N, Miller KM, Lazzerini-Denchi E, Sfeir A. Mammalian polymerase theta promotes alternative NHEJ and suppresses recombination. Nature 2015;518:254–7.
11. Murai J, Huang SY, Das BB, Renaud A, Zhang Y, Doroshow JH, et al. Trapping of PARP1 and PARP2 by clinical PARP inhibitors. Cancer Res 2012;72:5588–99.
12. Moynahan ME, Jasin M. Mitotic homologous recombination maintains genomic stability and suppresses tumorigenesis. Nat Rev Mol Cell Biol 2010;11:196–207.
13. Venkitaraman AR. Cancer suppression by the chromosome custodians, BRCA1 and BRCA2. Science 2014;343:1470–5.
14. Patel AG, Sarkaria JN, Kaufmann SH. Nonhomologous end joining drives poly(ADP-ribose) polymerase (PARP) inhibitor lethality in homologous recombination-deficient cells. Proc Natl Acad Sci U S A 2011;108:3406–11.
15. Menear KA, Adcock C, Boulter R, Cockcroft XL, Copsey L, Cranston A, et al. 4-[3-(4-cyclopropanecarbonylpiperazine-1-carbonyl)-4-fluorobenzyl]-2H-phthalazin-1-one: a novel bioavailable inhibitor of poly(ADP-ribose) polymerase-1. J Med Chem 2008;51:6581–91.
16. European Medicines Agency (EMA). Lynparza recommended for approval in ovarian cancer; 2014. Available from:http://www.ema.europa.eu/ema/index.jsp?curl=pages/news_and_events/news/2014/10/news_detail_002196.jsp&mid=WC0b01ac058004d5c1.

17. US Food and Drug Administration (FDA). FDA News release: FDA approves Lynparza to treat advanced ovarian cancer; 2014. Available from:http://www.fda.gov/NewsEvents/Newsroom/PressAnnouncements/ucm427554.htm.
18. Mullins DW Jr, Giri CP, Smulson M. Poly(adenosine diphosphate-ribose) polymerase: the distribution of a chromosome-associated enzyme within the chromatin substructure. Biochemistry 1977;16:506–13.
19. Fisher AE, Hochegger H, Takeda S, Caldecott KW. Poly(ADP-ribose) polymerase 1 accelerates single-strand break repair in concert with poly (ADP-ribose) glycohydrolase. Mol Cell Biol 2007;27:5597–605.
20. Audeh MW, Carmichael J, Penson RT, Friedlander M, Powell B, Bell-McGuinn KM, et al. Oral poly(ADP-ribose) polymerase inhibitor olaparib in patients with BRCA1 or BRCA2 mutations and recurrent ovarian cancer: a proof-of-concept trial. Lancet 2010;376:245–51.
21. Tutt A, Robson M, Garber JE, Domchek SM, Audeh MW, Weitzel JN, et al. Oral poly(ADP-ribose) polymerase inhibitor olaparib in patients with BRCA1 or BRCA2 mutations and advanced breast cancer: a proof-of-concept trial. Lancet 2010;376:235–44.
22. Gelmon KA, Tischkowitz M, Mackay H, Swenerton K, Robidoux A, Tonkin K, et al. Olaparib in patients with recurrent high-grade serous or poorly differentiated ovarian carcinoma or triple-negative breast cancer: a phase 2, multicentre, open-label, non-randomised study. Lancet Oncol 2011; 12:852–61.
23. Ledermann J, Harter P, Gourley C, Friedlander M, Vergote I, Rustin G, et al. Olaparib maintenance therapy in platinum-sensitive relapsed ovarian cancer. N Engl J Med 2012;366:1382–92.
24. Edwards SL, Brough R, Lord CJ, Natrajan R, Vatcheva R, Levine DA, et al. Resistance to therapy caused by intragenic deletion in BRCA2. Nature 2008;451:1111–5.
25. Bouwman P, Aly A, Escandell JM, Pieterse M, Bartkova J, van der Gulden H, et al. 53BP1 loss rescues BRCA1 deficiency and is associated with triple-negative and BRCA-mutated breast cancers. Nat Struct Mol Biol 2010;17: 688–95.
26. Bunting SF, Callen E, Wong N, Chen HT, Polato F, Gunn A, et al. 53BP1 inhibits homologous recombination in Brca1-deficient cells by blocking resection of DNA breaks. Cell 2010;141:243–54.
27. Xu G, Chapman JR, Brandsma I, Yuan J, Mistrik M, Bouwman P, et al. REV7 counteracts DNA double-strand break resection and affects PARP inhibition. Nature 2015;521:541–4.
28. Jaspers JE, Kersbergen A, Boon U, Sol W, van Deemter L, Zander SA, et al. Loss of 53BP1 causes PARP inhibitor resistance in Brca1-mutated mouse mammary tumors. Cancer Discov 2013;3:68–81.
29. Rottenberg S, Jaspers JE, Kersbergen A, van der Burg E, Nygren AO, Zander SA, et al. High sensitivity of BRCA1-deficient mammary tumors to the PARP inhibitor AZD2281 alone and in combination with platinum drugs. Proc Natl Acad Sci U S A 2008;105:17079–84.
30. Hay T, Matthews JR, Pietzka L, Lau A, Cranston A, Nygren AO, et al. Poly-(ADP-ribose) polymerase-1 inhibitor treatment regresses autochthonous Brca2/p53-mutant mammary tumors in vivo and delays tumor relapse in combination with carboplatin. Cancer Res 2009;69:3850–5.
31. Elstrodt F, Hollestelle A, Nagel JH, Gorin M, Wasielewski M, van den Ouweland A, et al. BRCA1 mutation analysis of 41 human breast cancer cell lines reveals three new deleterious mutants. Cancer Res 2006;66:41–5.
32. Breslin C, Clements PM, El-Khamisy SF, Petermann E, Iles N, Caldecott KW. Measurement of chromosomal DNA single-strand breaks and replication fork progression rates. Methods Enzymol 2006;409:410–25.
33. Rulten SL, Fisher AE, Robert I, Zuma MC, Rouleau M, Ju L, et al. PARP-3 and APLF function together to accelerate nonhomologous end-joining. Mol Cell 2011;41:33–45.
34. Liu X, Holstege H, van der Gulden H, Treur-Mulder M, Zevenhoven J, Velds A, et al. Somatic loss of BRCA1 and p53 in mice induces mammary tumors with features of human BRCA1-mutated basal-like breast cancer. Proc Natl Acad Sci U S A 2007;104:12111–6.
35. Ame JC, Rolli V, Schreiber V, Niedergang C, Apiou F, Decker P, et al. PARP-2, a novel mammalian DNA damage-dependent poly(ADP-ribose) polymerase. J Biol Chem 1999;274:17860–8.
36. Choi KH, Chen CJ, Kriegler M, Roninson IB. An altered pattern of cross-resistance in multidrug-resistant human cells results from spontaneous mutations in the mdr1 (P-glycoprotein) gene. Cell 1988;53: 519–29.
37. Evers B, Drost R, Schut E, de Bruin M, van der Burg E, Derksen PW, et al. Selective inhibition of BRCA2-deficient mammary tumor cell growth by AZD2281 and cisplatin. Clin Cancer Res 2008;14:3916–25.
38. Javle M, Curtin NJ. The role of PARP in DNA repair and its therapeutic exploitation. Br J Cancer 2011;105:1114–22.
39. Murai J, Zhang Y, Morris J, Ji J, Takeda S, Doroshow JH, et al. Rationale for poly(ADP-ribose) polymerase (PARP) inhibitors in combination therapy with camptothecins or temozolomide based on PARP trapping versus catalytic inhibition. J Pharmacol Exp Ther 2014;349:408–16.
40. Plummer ER, Middleton MR, Jones C, Olsen A, Hickson I, McHugh P, et al. Temozolomide pharmacodynamics in patients with metastatic melanoma: DNA damage and activity of repair enzymes O6-alkylguanine alkyltransferase and poly(ADP-ribose) polymerase-1. Clin Cancer Res 2005;11:3402–9.
41. Plummer R, Lorigan P, Evans J, Steven N, Middleton M, Wilson R, et al. First and final report of a phase II study of the poly(ADP-ribose) polymerase (PARP) inhibitor, AG014699, in combination with temozolomide (TMZ) in patients with metastatic malignant melanoma (MM). J Clin Oncol 24:18s, 2006 (suppl; abstr 8013).
42. Bonner WM, Redon CE, Dickey JS, Nakamura AJ, Sedelnikova OA, Solier S, et al. GammaH2AX and cancer. Nat Rev Cancer 2008;8:957–67.
43. Riballo E, Kuhne M, Rief N, Doherty A, Smith GC, Recio MJ, et al. A pathway of double-strand break rejoining dependent upon ATM, Artemis, and proteins locating to gamma-H2AX foci. Mol Cell 2004;16:715–24.
44. Mohrin M, Bourke E, Alexander D, Warr MR, Barry-Holson K, Le Beau MM, et al. Hematopoietic stem cell quiescence promotes error-prone DNA repair and mutagenesis. Cell Stem Cell 2010;7:174–85.
45. Milyavsky M, Gan OI, Trottier M, Komosa M, Tabach O, Notta F, et al. A distinctive DNA damage response in human hematopoietic stem cells reveals an apoptosis-independent role for p53 in self-renewal. Cell Stem Cell 2010;7:186–97.
46. Lane AA, Scadden DT. Stem cells and DNA damage: persist or perish? Cell 2010;142:360–2.
47. Lehtiö L, Jemth AS, Collins R, Loseva O, Johansson A, Markova N, et al. Structural basis for inhibitor specificity in human poly(ADP-ribose) polymerase-3. J Med Chem 2009;52:3108–11.
48. Loseva O, Jemth AS, Bryant HE, Schuler H, Lehtio L, Karlberg T, et al. PARP-3 is a mono-ADP-ribosylase that activates PARP-1 in the absence of DNA. J Biol Chem 2010;285:8054–60.
49. Wahlberg E, Karlberg T, Kouznetsova E, Markova N, Macchiarulo A, Thorsell AG, et al. Family-wide chemical profiling and structural analysis of PARP and tankyrase inhibitors. Nat Biotechnol 2012;30: 283–8.
50. Papeo G, Posteri H, Borghi D, Busel AA, Caprera F, Casale E, et al. Discovery of 2-[1-(4,4-difluorocyclohexyl)piperidin-4-yl]-6-fluoro-3-oxo-2,3-dihydro-1H-isoindole-4-carboxamide (NMS-P118): a potent, orally available, and highly selective PARP-1 inhibitor for cancer therapy. J Med Chem 2015;58:6875–98.